

Coherence lengths and neutron optics

D. Petrascheck

Institut für Theoretische Physik, Universität Linz, A-4040 Linz, Austria

(Received 25 November 1986)

The dynamical diffraction of divergent beams and its application to neutron interferometry are considered. The coherence properties of thermal neutrons are studied, and it is shown that the extreme anisotropy of dynamically diffracted wave packets should be included in the discussion of coherence lengths. Finally, the mechanism leading to a nondispersive phase shift is investigated.

I. INTRODUCTION

Wave packets are a convenient aid for visualizing the behavior of particles in optics. It is therefore challenging to demonstrate their dispersive propagation and their coherence properties for massive de Broglie waves as well. For such experiments time-resolved interferometry is needed.¹⁻³ To my knowledge all neutron interferometric experiments concerning the coherence length have hitherto been performed under the condition of a stationary incident beam. An exception is perhaps an experiment showing the interference patterns when the intensity in one path is diminished either by introducing an absorber or by periodic chopping.⁴

In the standard neutron interferometry experiment a phase shifter is brought into one of the two beams of the interferometer (see Fig. 1). The optical paths for the two beams thus become unequal, giving rise to intensity oscillations. Usually, these oscillations provide the coherent scattering length of the phase-shifting material. With increasing order the contrast of these oscillations decreases.^{5,6} This loss of contrast may be caused by the phase shifter (absorption, diffuse scattering, inhomogeneities, etc.) or by the wavelength spread. For the following considerations only the last point is of interest. The decrease of contrast with increasing optical path difference has been used by Kaiser, Werner, and George⁷ to measure the longitudinal coherence length of the neutron beam assuming Gaussian incident wave packets. It should be noted, that if one relates the coherence length of the wave packet to its width, the dispersive motion of the wave packet leads to increasing spatial extension without an increase of the coherence length.⁸ From a rigorous point of view, the knowledge of the wavelength distribution alone does not allow any conclusion about the shape of a wave packet.⁹

II. DIFFRACTION OF WAVE PACKETS

Consider the wave packet

$$\phi(\mathbf{x}, t) = \int \frac{d^3k}{(2\pi)^3} F(\mathbf{k}, \mathbf{k}_0) e^{i\mathbf{k}\cdot\mathbf{x} - i\omega_k t}, \tag{1}$$

which propagates in a force-free vacuum region. The wave packet is centered around the wave vector \mathbf{k}_0 . In neutron optics the width of the wave-number distribution

$\Delta k/k_0$ is usually of the order of 10^{-2} – 10^{-3} and the angular spread of the plane-wave components does not exceed a few degrees around \mathbf{k}_0 . If one wave packet per unit time is emitted from the neutron source, the total current measured by the detector is

$$I = \int d^3x |\phi(\mathbf{x}, t)|^2 = \int \frac{d^3k}{(2\pi)^3} |F(\mathbf{k}, \mathbf{k}_0)|^2, \tag{2}$$

which can be deduced from particle conservation. Equation (2) shows that the dispersive motion of wave packets resulting from $\omega_k = \hbar k^2/2m$, where m is the neutron mass, does not enter into neutron optics, even for the classical experiment in neutron interferometry, where two displaced wave packets $\phi = [\phi(\mathbf{x}, t) + \phi(\mathbf{x} - \mathbf{a}, t)]/2$ are brought to interference.⁵⁻⁸

We now assume that the wave packet Eq. (1) is incident on a single crystal plate under the condition of symmetrical Laue diffraction. We choose a system of coordinates with $\hat{\mathbf{e}}_z$ normal to the plate surface and $\hat{\mathbf{e}}_x$ along the reflecting reciprocal wave vector \mathbf{G} (see Fig. 1). The wave vector \mathbf{k}_0 of the center of the wave packet is assumed to lie in the x - z plane and to fulfill the Bragg condition exactly.

The dynamical diffraction of wave packets may be described by the dynamical diffraction of single plane waves

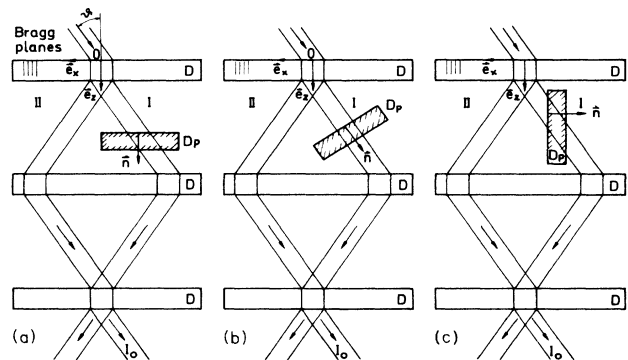


FIG. 1. Schematic diagram of a LLL interferometer. The wave front is delayed (accelerated) normal to phase shifter depending on the sign of the potential. (a) Dispersive phase shift; (b) longitudinal (dispersive) phase shift; (c) "nondispersive" phase shift.

$\psi_i = \exp(i\mathbf{k}\mathbf{x})$ that are superposed appropriately behind the crystal. If only integrated intensities are considered, one obtains

$$I_G = \int \frac{d^3k}{(2\pi)^3} |F(\mathbf{k}, \mathbf{k}_0)|^2 \frac{\sin^2[A(1+y^2)^{1/2}]}{1+y^2} \quad (3)$$

for the intensity of the beam diffracted by a single-crystal plate of thickness D . The notation used is similar to that of Ref. 10. $A = \pi D / \Delta$ is a dimensionless parameter that relates the thickness to the Pendellösung length $\Delta = \pi \hbar^2 k_z / m |V_G|$, where m is the neutron mass and V_G the Fourier transform of the interaction potential. The quantity

$$y = \Delta_0 \tan \theta_0 (k_x - k_{0x}) / \pi \quad (4)$$

known, mainly in the domain of electron diffraction, as the "Selektionsfehler," is a measure of the deviation from the exact Bragg condition in the component of the incident wave vector \mathbf{k} parallel to \mathbf{G} . Δ_0 and θ_0 are the Pendellösung or extinction length and Bragg angle, respectively, for the wave number k_0 of the center of the wave packet. It should be noted that $\Delta_0 \tan \theta_0$ is independent of the wavelength λ_0 and the mass m of the incident neutron. For some applications it therefore seems useful to introduce

$$\Lambda = \Delta_0 \tan \theta_0 / \pi = \hbar^2 G / 2m |V_G|$$

instead of Δ_0 as the characteristic dynamical diffraction length,^{11,12} since Λ depends only on the lattice parameters, the reflecting Bragg plane, the coherent scattering length b_c , and a small temperature-dependent contribution from the Debye-Waller factor.

The average intensity of a diffracted plane wave has the typical Lorentzian dependence on the parameters, which determines the range of acceptance of dynamical diffraction. This so-called "Bragg-window"¹³ selects a narrow wave-vector interval for the x component of \mathbf{k} . Assuming a Gaussian weighting function

$$F(\mathbf{k} - \mathbf{k}_0) = (2\pi/\sigma^2)^{3/4} \exp[-(\mathbf{k} - \mathbf{k}_0)^2 / 4\sigma^2] \quad (5)$$

one obtains approximately for thick crystals

$$I_G \simeq I_\sigma \left[\frac{\pi}{2} - \frac{1}{4} \left[\frac{\pi}{A_0} \right]^{1/2} e^{-2A_0 \delta \sigma_z^2} \cos \left[2A_0 + \frac{\pi}{4} \right] \right] \quad (6)$$

with

$$I_\sigma = \frac{1}{\sqrt{2\pi\Lambda\sigma}} \quad (7)$$

and $\sigma_z = \sigma / k_{0z}$. I_σ is introduced to normalize I_G in the usual manner¹⁰ and Eq. (7) holds only for a wave-vector spread σ much larger than the Bragg window. Thus I_G is much smaller than unity and expresses the fact that only a small part of the incident wave packet is diffracted

dynamically. The approximation for I_G , Eq. (6), neglects contributions of the order of $1/A_0$, where $A_0 = \pi D / \Delta_0$ is the thickness parameter for k_0 . When one chooses instead of Eq. (5) an anisotropic wave-vector distribution, then it becomes apparent that the attenuation of the Pendellösung oscillations depends only on the spread in the z component of \mathbf{k} .

III. TRIPLE LAUE CASE INTERFEROMETRY

Now we assume that the beam is incident on a Laue-Laue-Laue (LLL) interferometer in which a phase shifting slab is placed in one path of the interferometer (see Fig. 1) parallel to the interferometer crystal. According to Eq. (2) the intensity for the forward beam I_0 may be written as

$$I_0(\chi_0) = \int \frac{d^3k}{(2\pi)^3} |F(\mathbf{k}, \mathbf{k}_0) \psi_0^I(\mathbf{k}, \mathbf{r})(1 + e^{i\chi})|^2 \quad (8)$$

where ψ_0^I is the plane wave traveling along path I [see Fig. 1(a)] in the forward direction. The once transmitted and twice diffracted wave function reads¹⁴

$$\begin{aligned} \psi_0^I = & - \left\{ \cos[A(1+y^2)^{1/2}] + \frac{iy}{(1+y^2)^{1/2}} \sin[A(1+y^2)^{1/2}] \right\} \\ & \times \frac{\sin^2[A(1+y^2)^{1/2}]}{1+y^2} e^{i\mathbf{k}\mathbf{r} + i\phi_0}, \end{aligned} \quad (9)$$

where ϕ_0 is a phase angle which is not relevant for our considerations. The phase difference produced by the phase shifter is given by

$$\chi = (\mathbf{K} - \mathbf{k})\mathbf{n}D_p \simeq -2\pi N b_c D_p / k_z = \chi_0 k_{0z} / k_z, \quad (10)$$

where \mathbf{K} is the wave vector within the phase shifter differing from \mathbf{k} only in its component parallel to \mathbf{n} , the unit vector normal to the front surface [see Fig. 1(a)], D_p is the thickness of the phase shifter, N the density of the scattering atoms with a coherent scattering length b_c . In most cases absorption and diffuse scattering do not lead to an essential reduction of the contrast. However, if there is appreciable elastic scattering from small crystallites and/or inhomogeneities, the attenuation of the beam becomes important.¹² It may then be taken into account in a crude fashion by means of an imaginary part of the scattering length b_c and the phase shift χ_0 : $b_c = b' - ib''$, $\chi_0 = \chi'_0 + i\chi''_0$.

Equation (8) is evaluated for thick crystals using the same method as for a single crystal. The result is

$$I_0(\chi_0) = I_a(\chi_0) + I_1(\chi_0) + 2I_2(\chi_0) + I_3(\chi_0) \quad (11)$$

with

$$I_a(\chi_0) = I_\sigma \frac{9\pi}{64} e^{-\chi''_0} (\cosh \chi''_0 + e^{-\sigma_z^2 \chi_0'^2 / 2} \cos \chi'_0) \quad (12)$$

and

$$\begin{aligned} I_m(\chi_0) = & - \frac{I_\sigma}{32} e^{-\chi''_0} \left[\frac{\pi}{m A_0} \right]^{1/2} \left[2e^{-2m^2 A_0^2 \sigma_z^2} \cos \left[2m A_0 + \frac{\pi}{4} \right] \cosh \chi''_0 + e^{-(2m A_0 + \chi'_0)^2 \sigma_z^2 / 2} \cos \left[2m A_0 + \chi'_0 + \frac{\pi}{4} \right] \right. \\ & \left. + e^{-(2m A_0 - \chi'_0)^2 \sigma_z^2 / 2} \cos \left[2m A_0 - \chi'_0 + \frac{\pi}{4} \right] \right] \end{aligned} \quad (13)$$

for $m = 1, 2$, and 3 . I_a describes the decrease of the intensity oscillations of the average, thickness-independent part with increasing χ_0 . The dependence of b'' and χ'' on \mathbf{k} is neglected, because it leads to contributions of the order $(\sigma\chi_0''/k_0)^2$ which are small compared to χ_0'' .

The corrections for the finite thickness of the interferometer crystal are contained in Eq. (13). A special situation occurs for $\chi_0 \approx 2mA_0$ and $\chi_0\sigma_z > 1$. The latter condition implies that the oscillation of I_a are already suppressed, whereas from the former condition it is seen that the last term of Eq. (13) contributes to the interference oscillations. This small increase of the fringe visibility has not yet been observed; it could be considered as a "phase echo" at the interferometer from the phase shifter.

For studying the longitudinal coherence length of the neutron beam, the phase shifter is placed in the interferometer perpendicular to the beam, as shown in Fig.

$$I_m = -\frac{I_\sigma}{32} \left[\frac{\pi}{mA_0} \right]^{1/2} e^{-\chi_0''} \left[2e^{-2(mA_0\sigma_z)^2} \cos \left[2mA_0 + \frac{\pi}{4} \right] \cosh\chi_0'' + e^{-\sigma_z^2(2mA_0 + \chi_0' \cos^2\theta_0)^2/2} \cos \left[2mA_0 + \chi_0' + \frac{\pi}{4} \right] + e^{-\sigma_z^2(2mA_0 - \chi_0' \cos^2\theta_0)^2/2} \cos \left[2mA_0 - \chi_0' + \frac{\pi}{4} \right] \right]. \quad (16)$$

For a typical neutron interferometer with crystal slabs of a few millimeters and customary values of the wavelength spread and the reduced thickness A_0 , the corrections shown in Eq. (16) are less than 1%. Therefore, Eq. (15) is the basis for the explanation of the classical experiment for measuring the longitudinal coherence length by Kaiser, Werner, and George described in Ref. 7. These authors used an aluminum phase shifter in their experiment with a path difference $|a| = |\chi_0'/k_0| = \lambda_0^2 b' ND_p / 2\pi$, i.e., 54 Å per cm for neutrons with $\lambda_0 = 1.268$ Å.

Figure 2, which is adapted from Ref. 7, shows the loss of contrast with increasing thickness of the Al phase shifter. The experiment was designed to demonstrate the uncertainty explicitly. The uncertainty in the relative position of two wave packets traveling along paths I and II, respectively, is calculated via the width of the Gaussian in Fig. 2, although the enhanced intensity in the tails indicates a somewhat larger variance.¹⁵

The experimental results can be evaluated using Eq. (15) with $\chi_0'' = 0$. Rewriting the parameter in the exponent of Eq. (15) one obtains

$$\sigma_z \chi_0 \cos^2\theta_0 = \sigma a_z,$$

$$I_a(\chi_0) = \frac{9\pi}{64} I_\sigma e^{-\chi_0''} \left[\cosh\chi_0'' + \left| 1 + \frac{2\pi\Delta t}{\Delta_0} - \frac{5}{9} \left[\frac{2\pi\Delta t}{\Delta_0} \right]^2 \right| e^{-2\pi\Delta t/\Delta_0} \cos\chi_0' \right] \quad \text{for } \Delta t > 0, \quad (19)$$

a result already known from the defocused interferometer.¹⁴ $I_0(\chi_0)$ is displayed in Fig. 4 for $\chi_0'' = 0$. A path shift comparable to the macroscopic size Δ_0 cannot be reached via the refraction index of phase shifting materials, and no

1(b). According to Eq. (10) the phase shift is now given by

$$\chi \approx -2\pi N b_c D_p / (k_z \cos\theta_0 - k_x \sin\theta_0) \approx \chi_0 \left[1 - \frac{k_z - k_{0z}}{k_{0z}} \cos^2\theta_0 \right] \quad (14)$$

with $\chi_0 = -\lambda_0 N b_c D_p$, the longitudinal phase difference between the two beams. Since the "Bragg window" restricts the wave vectors parallel to \mathbf{G} , the variation of k_x can be neglected in Eq. (14).

When carrying out the calculations completely analogous to the former case one has to substitute in Eq. (11)

$$I_a(\chi_0) = I_\sigma \frac{9\pi}{64} e^{-\chi_0''} (\cosh\chi_0'' + e^{-\sigma_z^2 \chi_0'^2 \cos^4\theta_0/2} \cos\chi_0') \quad (15)$$

and

where $a_z = a \cos\theta_0$ is the path difference along the z direction. In a one-dimensional model,⁷ where only the path difference a occurs, it has to be combined with the variance $\sigma_f \approx \sigma \cos\theta_0$ measured behind the interferometer, to give the above result.

The physically most interesting situation arises from a phase shift parallel to \mathbf{G} as shown in Fig. 1(c). There one obtains

$$\chi = 2\pi N b_c D_p / k_x = \chi_0 - 2\pi y \Delta t / \Delta_0 \quad (17)$$

for the phase shift with $\chi_0 = -\lambda_0 N b_c D_p / \sin\theta_0$ and

$$\Delta t = \lambda_0^2 N b' D_p \cos\theta_0 / 4\pi \sin^3\theta_0. \quad (18)$$

It should be mentioned that Δt may be obtained from ray optical considerations taking into account the small lateral displacement of the rays caused by the phase shifter. According to Fig. 3, Δt is given by Eq. (18) and the situation that arises from the displacement of the rays is exactly the same as for a defocused interferometer.¹⁴ Assuming sufficiently thick crystals I_m may be neglected. For the average intensity, σ_z has no effect on the oscillations. Therefore one obtains

reduction of the contrast due to the divergence of the incident beam is expected. Although phase shifters in the nondispersive position evidently show higher contrast than in the dispersive one, the observed reduction of con-

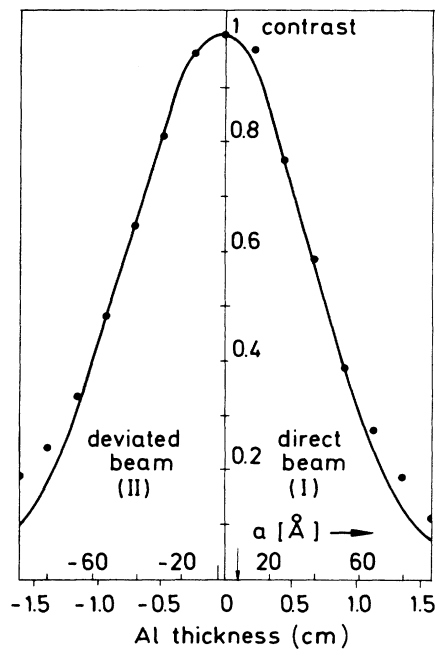


FIG. 2. Loss of contrast when the Al phase shifter is placed in the interferometer normal to the beam [see Fig. 1(b)]. The contrast $C_0 = (I_{\max} - I_{\min}) / (I_{\max} + I_{\min})$ is corrected for inhomogeneities, thickness variations, and wave amplitude attenuation and is normalized to 1 at the peak. The solid line is a Gaussian passing through most of the data points. It is centered at $a = -4 \text{ \AA}$, reflecting the fact that the two beams are not precisely equal. The figure is adapted from Kaiser, Werner, and George (Ref. 7).

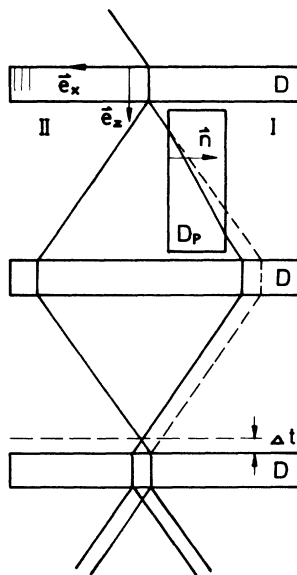


FIG. 3. Optical ray trajectories for a nondispersive phase shifter. The situation corresponds to a defocus Δt .

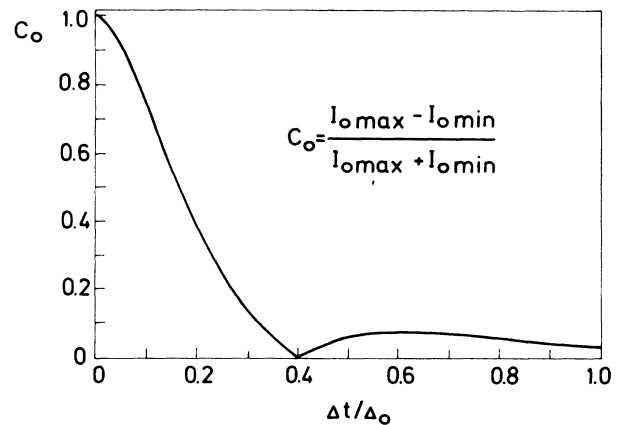


FIG. 4. Loss of contrast for a nondispersive interferometer ($\chi''_0 = 0$). The contrast is $\frac{1}{2}$ for $\Delta t \sim 0.16\Delta_0$.

trast is stronger than displayed in Fig. 4.^{12,16} Small angle scattering, elastic scattering by small crystallites and thickness variations cause a higher reduction of the contrast than expected from the wavelength spread.

IV. SUMMARY

We have applied dynamical diffraction theory to a polychromatic beam of thermal neutrons. The calculations, which were carried out explicitly for an incident Gaussian wave-vector distribution show that the dynamically diffracted intensity fraction is proportional to $1/\sigma\Lambda$, where Λ is a characteristic reflection length and σ the width of the wave-vector distribution. Since Λ is wave-number independent, σ alone determines the total diffracted intensity. Extending the calculations to the neutron interferometer we show that this modifies the shape of the incident Gaussian wave packets.

One has to distinguish coherence lengths parallel and perpendicular to the relevant Bragg vector \mathbf{G} , instead of longitudinal and transversal coherence lengths with respect to \mathbf{k}_0 . Therefore, the macroscopic coherence length mentioned in Ref. 13 does not appear in our calculations for the direction normal to the crystal plates. In addition, our results show that the frequently used one-dimensional model is too simple for a sufficient explanation of the coherence properties.

Finally the attenuation of the contrast with increasing nondispersive phase shift¹² is estimated theoretically. The results are consistent with a simple ray optical model. The results may suggest ways to increase the accuracy in measuring neutron scattering lengths.

ACKNOWLEDGMENTS

The author wishes to thank Professor U. M. Titulaer and Professor H. Rauch for many helpful discussions. The work was supported by the Fonds zur Förderung der Wissenschaftlichen Forschung, Project No. S42/01.

- ¹H. Kaiser, S. A. Werner, and E. A. George, *Phys. Rev. Lett.* **51**, 1106 (1983).
- ²A. G. Klein and G. I. Opat, *J. Phys. (Paris) Colloq.* **45**, C3-235 (1984).
- ³W. A. Hamilton, A. G. Klein, and G. I. Opat, *Phys. Rev. A* **28**, 3149 (1983).
- ⁴H. Rauch and J. Summhammer, *Phys. Lett. A* **104**, 44 (1984).
- ⁵H. Rauch and M. Suda, *Phys. Status Solidi A* **25**, 495 (1974).
- ⁶H. Rauch, in *Neutron Interferometry*, edited by U. Bouse and H. Rauch (Oxford University Press, Oxford, 1979), p. 161.
- ⁷H. Kaiser, S. A. Werner, and E. A. George, *Phys. Rev. Lett.* **50**, 560 (1983).
- ⁸A. G. Klein, G. I. Opat, and W. A. Hamilton, *Phys. Rev. Lett.* **50**, 563 (1983).
- ⁹G. Comsa, *Phys. Rev. Lett.* **51**, 1105 (1983).
- ¹⁰H. Rauch and D. Petrascheck, in *Neutron Diffraction*, Vol. 6 of *Topics in Current Physics*, edited by H. Dachs (Springer, Berlin, 1978), p. 303.
- ¹¹M. A. Horne and J. Arthur, *Phys. Rev. B* **32**, 5747 (1985).
- ¹²H. Rauch, E. Seidl, D. Tuppinger, D. Petrascheck, and R. Scherm, *Z. Phys.* (to be published).
- ¹³D. M. Greenberger, *Rev. Mod. Phys.* **55**, 875 (1983).
- ¹⁴D. Petrascheck and R. Folk, *Phys. Status Solidi A* **36**, 147 (1976).
- ¹⁵J. B. M. Uffink, *Phys. Lett.* **108A**, 59 (1985).
- ¹⁶H. Rauch and D. Tuppinger, *Z. Phys. A* **322**, 427 (1985).